

## Possible triaxial structures in $^{24}\text{Mg}$ from $^{16}\text{O} + ^{24}\text{Mg}$ elastic and inelastic scattering

J. S. Eck

*Department of Physics, Kansas State University, Manhattan, Kansas, 66506  
and Department of Nuclear Physics, Australian National University, Canberra, ACT 2600, Australia*

J. Nurzynski, T. R. Ophel, P. D. Clark, D. F. Hebbard, and D. C. Weisser

*Department of Nuclear Physics, Australian National University, Canberra, ACT 2600, Australia*

(Received 10 September 1980)

The energy level scheme for the low-lying collective levels of  $^{24}\text{Mg}$  are reasonably described by an asymmetric rotor with  $\beta_2 = 0.52$  and  $\gamma = 22^\circ$ . To further investigate possible triaxial structures in  $^{24}\text{Mg}$ , we have measured elastic and inelastic scattering angular distributions for excitation of the lowest three excited states in  $^{24}\text{Mg}$  at an  $^{16}\text{O}$  bombarding energy of 67 MeV in the angular range  $\theta_{\text{c.m.}} = 10\text{--}65^\circ$ . The measured cross sections have been analyzed using coupled channels calculations assuming that  $^{24}\text{Mg}$  behaves as (1) a symmetric rotor and (2) a triaxial rotor. Because of the fact that the  $2_2^+$  and  $4_1^+$  states in  $^{24}\text{Mg}$  are unresolved, difficulty occurs in distinguishing between the two models. Considering  $^{24}\text{Mg}$  to be a triaxial rotor, however, does yield a simple description of the bound states and scattering to the low-lying collective levels.

NUCLEAR REACTIONS  $^{24}\text{Mg}(^{16}\text{O}, ^{16}\text{O})^{24}\text{Mg}^*$  elastic and inelastic scattering  $Q = 0.00, -1.37, -4.12, \text{ and } -4.23$  MeV at  $E(^{16}\text{O}) = 67$  MeV. Measured  $\sigma_{\text{el}}(\theta)$  and  $\sigma_{\text{inel}}(\theta)$  for  $\theta_{\text{c.m.}} = 10\text{--}65^\circ$ , calculated  $\sigma_{\text{el}}(\theta)$  and  $\sigma_{\text{inel}}(\theta)$  using coupled channels and symmetric and triaxial rotor models.

### I. INTRODUCTION

There have been many recent studies and determinations of the nuclear shape parameters of the low-lying collective levels of light nuclei from elastic and inelastic scattering measurements using coupled channels analysis.<sup>1-6</sup> In general, the nucleus under investigation is usually considered to have axial symmetry. Recently, coupled channels analyses of elastic and inelastic cross section data for the system  $^{12}\text{C} + ^{194}\text{Pt}$  have been carried out in which it was assumed that  $^{194}\text{Pt}$  is an asymmetric rotor.<sup>7</sup> A quite satisfactory fit to the inelastic cross sections was obtained using this scheme as long as hexadecapole deformation was included in the asymmetric rotor model.<sup>7</sup> It has been known for some time that in light nuclei, Hartree-Fock calculations<sup>8-10</sup> predict a triaxial deformation for the ground state rotational band of  $^{24}\text{Mg}$ . To investigate this possibility further, we have measured the elastic scattering cross section and the inelastic scattering cross section to the  $2_1^+$  ( $Q = -1.37$  MeV),  $4_1^+$  ( $Q = -4.12$  MeV), and  $2_2^+$  ( $Q = -4.23$  MeV) states in  $^{24}\text{Mg}$  for the system  $^{16}\text{O} + ^{24}\text{Mg}$  at an  $^{16}\text{O}$  bombarding energy of 67 MeV. The experimental details are given in Sec. II. The measured cross sections were analyzed assuming an asymmetric rotor model for the low-lying collective levels of  $^{24}\text{Mg}$ . The deformation parameters are determined from fitting the bound states of  $^{24}\text{Mg}$  using the Davydov-Filippov model<sup>11</sup>

for a triaxial rotor. The comparison of these results to those obtained assuming that  $^{24}\text{Mg}$  is a symmetric rotor are given in Sec. III. The results and conclusions of the present study are given in Sec. IV.

### II. EXPERIMENTAL PROCEDURE

The  $^{16}\text{O}$  beam was obtained from the Australian National University (ANU) sputter source and accelerated using the ANU 14UD tandem accelerator. The targets consisted of  $\sim 100$   $\mu\text{g}/\text{cm}^2$  Mg (greater than 99% enriched in  $^{24}\text{Mg}$ ) evaporated onto thin carbon foils. The scattered  $^{16}\text{O}$  were detected using the Enge split pole spectrograph and focal plane detector.<sup>12</sup> The data were recorded in the event mode and an energy, energy loss, position, and angle signal were recorded for each event.<sup>12</sup> The final spectra were obtained by gating the position spectrum on the  $^{16}\text{O}$  mass signal. The cross sections were absolutely normalized to Rutherford scattering by measuring the elastic scattering cross section at forward angles at an energy of  $E(^{16}\text{O}) = 35$  MeV. The absolute normalization is accurate to 10%. The measured cross sections are shown in Fig. 1. The  $2_2^+$  and  $4_1^+$  states are unresolved, and therefore their cross section is shown as a sum for these two states.

### III. ANALYSIS

Initially the elastic scattering cross section was fitted using a spherical optical model of the

Woods-Saxon form factor. The parameters were chosen to be those obtained by Cramer *et al.*,<sup>13</sup> to describe  $^{16}\text{O} + ^{28}\text{Si}$  scattering in the energy range from 33–201 MeV. These parameters are given by  $U = 10.00$  MeV,  $r_0 = 1.35$  fm,  $a = 0.618$  fm,  $W = 23.40$  MeV,  $r_w = 1.23$  fm,  $a_w = 0.552$  fm, and  $r_C = 1.35$  fm. This fit is not explicitly shown but is essentially identical to the fit to the elastic scattering cross section obtained using the coupled channels analysis shown in Fig. 1. Again the fit is quite good except for the angular region near  $60^\circ$  in which structure is beginning to appear in the elastic scattering cross section.

The potential for an asymmetric rotor<sup>7</sup> is given by

$$U(R) = Vf(R_0, a_0) + iWf(R_w, a_w), \quad (1)$$

where

$$f(R', a') = \frac{1}{1 + \exp[(R - R')/a']}, \quad (2)$$

$$R' = R_0 \left\{ 1 + \beta_{20} Y_{20}(\theta, \phi) + \beta_{22} [Y_{22}(\theta, \phi) + Y_{2-2}(\theta, \phi)] \right. \\ \left. + \beta_{40} Y_{40}(\theta, \phi) + \beta_{42} [Y_{42}(\theta, \phi) + Y_{4-2}(\theta, \phi)] \right. \\ \left. + \beta_{44} [Y_{44}(\theta, \phi) + Y_{4-4}(\theta, \phi)] \right\}. \quad (3)$$

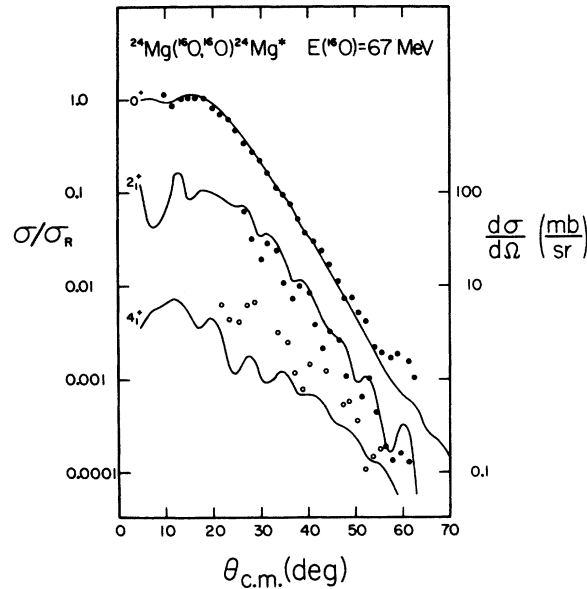


FIG. 1. Measured [indicated by solid dots for elastic scattering, crossed circles for scattering to the 1.37 MeV ( $2_1^+$ ) state, and open circles for scattering to the unresolved 4.12 MeV ( $4_1^+$ ) and 4.23 MeV ( $2_2^+$ ) states] and fitted (solid curves) differential cross sections for  $^{16}\text{O} + ^{24}\text{Mg}$  scattering at  $E(^{16}\text{O}) = 67$  MeV. The elastic scattering is given as the ratio-to-Rutherford scattering and is indicated by the left hand scale, while the inelastic cross sections are given in mb/sr as indicated by the right hand scale. The solid curves are fits assuming a symmetric rotor model for  $^{24}\text{Mg}$  with  $\beta_2 = 0.36$  and  $\beta_4 = -0.10$ . See text for details.

In the present work  $\beta_{42} = \beta_{44} = 0$ . In the usual parametrization<sup>14</sup> of a triaxial rotor  $\beta_{20} = \beta \cos \gamma$  and  $\beta_{22} = (1/\sqrt{2})\beta \sin \gamma$ , and the parameters  $\beta$  and  $\gamma$  are employed rather than  $\beta_{20}$  and  $\beta_{22}$ . The value of  $\gamma$  was obtained in the present work by fitting the low-lying energy levels of  $^{24}\text{Mg}$  using the Davydov-Filippov model of a triaxial rotor.

From Davydov *et al.*,<sup>11</sup> the ratio of the energy of the second  $2^+$  state to that of the first  $2^+$  state is given by

$$R = \frac{\epsilon_2(2)}{\epsilon_1(2)} = \frac{1 + (1 - \frac{8}{9} \sin^2 3\gamma)^{1/2}}{1 - (1 - \frac{8}{9} \sin^2 3\gamma)^{1/2}}. \quad (4)$$

For  $^{24}\text{Mg}$ ,  $\epsilon_2(2) = 4.23$  MeV and  $\epsilon_1(2) = 1.37$  MeV, yielding  $\gamma = 21.9^\circ \approx 22^\circ$ . The energy levels in  $^{24}\text{Mg}$  can be calculated from the work of DeMille *et al.*,<sup>15</sup> in which the energy levels of a triaxial rotor are plotted as a function of  $\gamma$ . For  $^{24}\text{Mg}$  the calculated and experimental energy levels<sup>16</sup> are shown in Fig. 2 and it is seen that they agree quite well for a value of  $\gamma = 22^\circ$ .

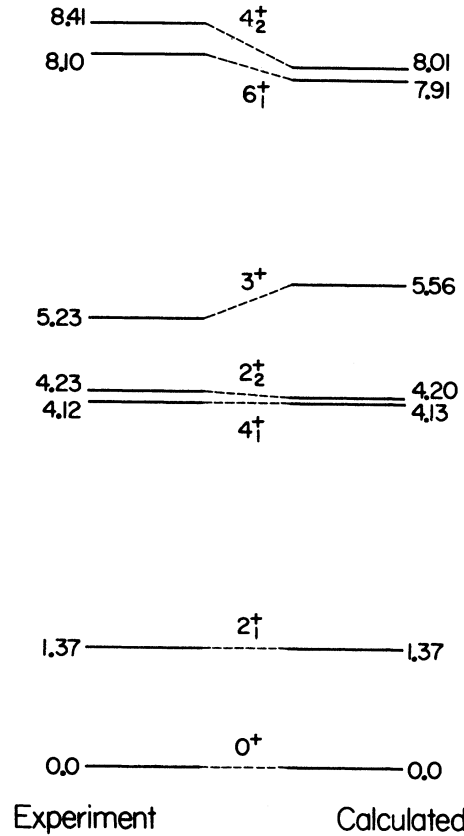


FIG. 2. Experimental and calculated energy levels of  $^{24}\text{Mg}$ . The experimental levels are from Ref. 16. The calculated levels were arrived at by assuming that  $^{24}\text{Mg}$  is an asymmetric rotor with  $\gamma = 22^\circ$  and  $\beta = 0.56$  using the Davydov-Filippov model and the calculated curves of Ref. 15.

The coupled channels calculations were performed using computer code ECIS.<sup>17</sup> The deformed optical potential was of the form

$$V = \frac{-V_0}{1 + \exp[(r - R'_0)/a_0]} \frac{-iW_0}{1 + \exp[(r - R'_w)/a_w]} + V_C(r), \quad (5)$$

where

$$R'_i(\theta, \phi) = R_{i0} [1 + \beta \cos \gamma Y_2^0 + (\frac{1}{2})^{1/2} \beta \sin \gamma (Y_2^{-2} + Y_2^{-2}) + \beta_4 Y_4^0], \quad (6)$$

where  $i = 0$  or  $w$ .

The Coulomb potential  $V_C(R_C)$  is generated from the deformed charge density

$$\zeta(r, \theta) = \zeta_0, \quad r \leq R_C(\theta) \\ = 0, \quad r > R_C(\theta),$$

where  $R_C(\theta) = r_C A_t^{1/3} (1 + \beta_2^C Y_2^0)$  fm and the charge density is normalized to  $Ze$ . The parametrization of  $R_C$  by  $A_t^{1/3}$ , rather than by  $(A_t^{1/3} + A_p^{1/3})$ , has been shown to give a better description of the double-folded Coulomb potential of the two heavy ions.<sup>18</sup> In the present calculations  $\beta_2^C = 0.498$ , and was chosen to reproduce the experimental  $B(E2)$  values for excitation of the  $2_1^+$  state in  $^{24}\text{Mg}$ .<sup>5</sup>

The initial calculations were made assuming that  $^{24}\text{Mg}$  is an axially symmetric rotor. In Eq. (6) this is equivalent to setting  $\gamma = 0.0$ . Using deformation parameters similar to those of Thompson and Eck<sup>19,20</sup> to fit  $^{16}\text{O} + ^{24}\text{Mg}$  scattering data at lower energy ( $\beta = 0.36$ ,  $\beta_4 = -0.10$ ), the fit to the scattering cross sections shown in Fig. 1 is obtained. The real and imaginary potential parameters were set equal. In using this model to fit the data presented here we are assuming that the measured cross section for scattering to the unresolved  $2_2^+$  and  $4_1^+$  states is solely due to the  $4_1^+$  state. Although the description of the elastic scattering cross section and the cross section for scattering to the  $2_1^+$  state is quite adequate, the calculated cross section to the  $4_1^+$  state lies considerably lower than the measured cross section for the combined  $2_1^+$  and  $4_1^+$  states, suggesting a considerable contribution from the  $2_2^+$  state.

Since the  $2_2^+$  state is not contained in the symmetric rotor model, we performed a coupled channels calculation assuming  $^{24}\text{Mg}$  to be an asymmetric rotor with  $\gamma = 22^\circ$  in agreement with the fit to the bound state levels of  $^{24}\text{Mg}$ . Initially we set  $\beta_4 = 0$  and fitted the cross sections assuming the combined  $4_1^+$  and  $2_2^+$  cross section is due solely to the  $2_2^+$  state. Using a value of  $\beta = 0.36$  and  $\gamma = 22^\circ$ , fits essentially identical to those shown in Fig. 3 are obtained for the  $0^+$  and  $2_1^+$  state cross sections.

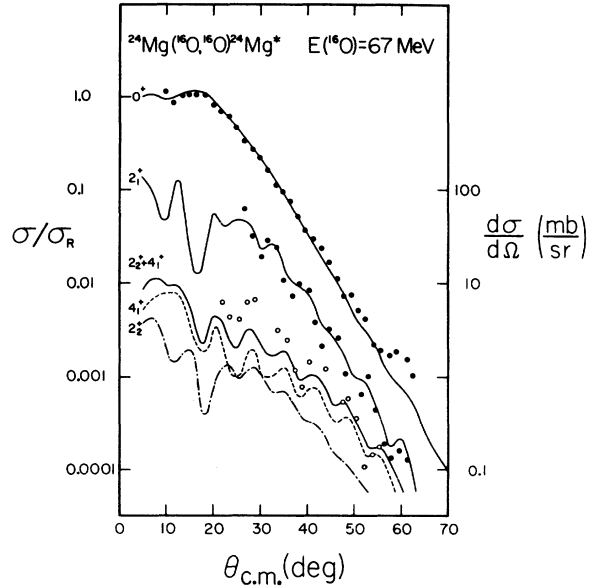


FIG. 3. Measured [indicated by solid dots for elastic scattering, crossed dots for scattering to the 1.37 MeV ( $2^+$ ) state, and open circles for scattering to the unresolved 4.12 MeV ( $4_1^+$ ) and 4.23 ( $2_2^+$ ) states] and fitted (solid, dashed, and dot-dashed lines) differential cross sections for  $^{16}\text{O} + ^{24}\text{Mg}$  scattering at  $E(^{16}\text{O}) = 67$  MeV. The elastic scattering is given as the ratio-to-Rutherford scattering as indicated by the left hand scale, while the inelastic cross sections are given in mb/sr as indicated by the right hand scale. The calculated cross sections correspond to (a)  $\beta = 0.36$ ,  $\gamma = 22^\circ$ , and  $\beta_4 = 0$ . In this case the fits to the  $0_1^+$  and  $2_1^+$  cross sections are given by the uppermost solid curves while the fit to the combined  $2_2^+ + 4_1^+$  cross section is given by the dot-dashed curve (labeled  $2_2^+$ ). (b)  $\beta = 0.36$ ,  $\gamma = 22^\circ$ , and  $\beta_4 = -0.10$ . In this case the fits to the  $0_1^+$  and  $2_1^+$  cross sections are identical to (a). The calculated cross section for excitation of the  $2_2^+$  state is identical to (a) and for excitation of the  $4_1^+$  state is shown by the dashed curve. The sum of the calculated  $2_2^+$  and  $4_1^+$  cross sections is shown by the lowest solid curve. See text for details.

The fit to the  $2_1^+$  state cross section is shown by the dot-dashed line in Fig. 3 for this case and remains essentially unaltered by including the  $4_1^+$  state in the calculations. Again the calculated cross section lies lower than the measured cross section and indicates the necessity of including the  $4_1^+$  state in the calculation.

In order to include the  $4_1^+$  state in the coupled channels calculations it is necessary to first calculate the mixing parameters (i.e., wave functions). In the usual  $|JMK\rangle$  basis the wave function of any state is

$$\Psi_{JM}^\alpha = \sum_{K=0}^J C_{JK}^\alpha |JMK\rangle,$$

where  $\alpha$  is a label to distinguish between  $2_1^+$  and  $2_2^+$  states. For the ground state  $J=0$ , so  $K=0$  and  $C_{00}^\alpha=1$ . For  $J=2$  states,  $K=0$  or  $2$ . Since  $(C_{20}^\alpha)^2 + (C_{22}^\alpha)^2=1$ , one mixing parameter is needed and this is defined as

$$B(T1) = \tan^{-1} \frac{C_{22}^\alpha}{C_{20}^\alpha}.$$

For  $J=4$  states,  $K=0, 2$ , or  $4$ . Since  $\sum_k (C_{4k}^\alpha)^2=1$ , two mixing parameters are needed and these are defined as

$$B(T1) = \tan^{-1} \frac{C_{42}^\alpha}{C_{40}^\alpha},$$

$$B(T2) = \tan^{-1} \frac{C_{44}^\alpha}{C_{42}^\alpha}.$$

Using the method of Baker *et al.*,<sup>7</sup> the mixing parameters were calculated for  $^{24}\text{Mg}$  using the parameters  $\beta=0.56$ ,  $\beta_4=-0.02$ , and  $\gamma=22^\circ$ . For the  $2_1^+$  state  $B(T1)=7.36^\circ$ , for the  $2_2^+$  state  $B(T1)=-82.64^\circ$ , and for the  $4_1^+$  state  $B(T1)=22.89^\circ$  and  $B(T2)=2.73^\circ$ . Using these values of mixing parameters and a value of  $\beta=0.36$ ,  $\beta_4=-0.10$ , and  $\gamma=22^\circ$ , the fits to the measured cross sections shown in Fig. 3 are obtained. The real and imaginary potential deformation parameters were set equal. The dashed curve is the calculated cross section for excitation of the  $4_1^+$  state and the dot-dashed curve is the calculated cross section for excitation of the  $2_2^+$  state, while the lowest solid curve is the sum of these two calculated cross sections. The values of  $\beta$  and  $\beta_4$  are different here because they represent the deformation parameters of the potential while those used in the calculation of the mixing coefficients are the intrinsic deformations of the  $^{24}\text{Mg}$  nucleus.<sup>21</sup>

The calculated cross sections give a fairly good representation of the data and the inclusion of both the  $2_2^+$  and  $4_1^+$  states gives considerable improvement in the angular range  $20-40^\circ$ , where  $(d\sigma/d\Omega)_{2_2^+}$  is approximately equal in magnitude to  $(d\sigma/d\Omega)_{4_1^+}$ . The structure in the calculated cross section is in fair agreement with the structure in the measured  $2_2^+$  and  $4_1^+$  cross section, although the magnitude of the calculated cross section for the sum of the  $2_2^+$  and  $4_1^+$  states is too low in the forward angle region.

The scattering of  $\alpha$  particles to the low-lying levels of  $^{24}\text{Mg}$  was considered earlier by Tamura.<sup>22</sup> He assumed a rotational vibrational model in which the  $0_1^+$ ,  $2_1^+$ ,  $4_1^+$ , and  $6_1^+$  are members of a  $K=0$  ground band and the  $2_2^+$  and  $3_1^+$  states are

members of the  $K=2$   $\gamma$ -vibrational band. Fits of similar quality to those presented here were obtained for the  $^{24}\text{Mg}(\alpha, \alpha^1)^{24}\text{Mg}^*$  cross sections at  $E_\alpha=28.5$  MeV. Although the measured cross section for the excitation of the  $3_1^+$  state was fairly inaccurate, it was found to place severe restraints on the acceptable parameters used in the coupled channels calculations of the inelastic  $\alpha + ^{24}\text{Mg}$  cross sections. Unfortunately, in the present work the cross section for population of the  $3_1^+$  state was not measured, as the yield is small and was not observed.

Recently the low-lying levels of  $^{26}\text{Mg}$  have been investigated<sup>23</sup> using  $^3\text{He} + ^{26}\text{Mg}$  inelastic scattering cross section data. In this case the low-lying levels of  $^{26}\text{Mg}$  were considered using a rotation-vibration model, and the calculated cross sections were in only fair agreement with the measured cross sections. Although the Hartree-Fock calculations<sup>8-10</sup> predict possible triaxial structures for  $2s-1d$  shell nuclei, the interpretation of measured inelastic scattering cross sections using nuclear models which include triaxial deformations has met with only limited success.

#### IV. CONCLUSIONS

The triaxial rotor model has been used to describe the low-lying collective levels of  $^{24}\text{Mg}$ . Coupled channels calculations incorporating the triaxial rotor model have been carried out in order to calculate the cross sections for population of the  $0^+$  (0.0),  $2_1^+$  (1.36),  $2_2^+$  (4.18), and  $4_1^+$  (4.23) states in  $^{24}\text{Mg}$  by scattering of  $^{16}\text{O}$  at a  $^{16}\text{O}$  bombarding energy of 67 MeV. Using previously determined deformation parameters and a value of  $\gamma$  which yields the optimum fit to the bound state energy levels, an improved description of the measured cross sections is obtained from that obtained using an axially symmetric rotor model description of  $^{24}\text{Mg}$ . Because the quality of the fits obtained is not ideal, it is difficult to draw any strong conclusions concerning triaxial structure in  $^{24}\text{Mg}$ ; however, the present results are consistent with this possibility. An advantage of using the triaxial rotor model to describe the  $^{16}\text{O} + ^{24}\text{Mg}$  scattering data is that the  $2_2^+$  and  $4_1^+$  are included within a single model framework.

This research supported in part by the Division of Chemical Sciences, U.S. Department of Energy, and the U.S. National Science Foundation under the U.S.-Australia Cooperative Science Program.

- <sup>1</sup>E. E. Gross, T. P. Cleary, J. L. C. Ford, D. C. Hensley, and K. S. Toth, *Phys. Rev. C* **17**, 1665 (1978).
- <sup>2</sup>Y. Lee, J. X. Saladin, J. Halden, J. O'Brien, C. Bakdash, C. Bemis, Jr., P. H. Stelson, F. K. McGowan, W. T. Miller, J. L. C. Ford, Jr., R. L. Robinson, and W. Tuttle, *Phys. Rev. C* **12**, 1483 (1975).
- <sup>3</sup>J. X. Saladin, I. Y. Lee, R. C. Haight, and D. Vitroux, *Phys. Rev. C* **14**, 992 (1976).
- <sup>4</sup>D. S. Gale and J. S. Eck, *Phys. Rev. C* **7**, 1950 (1973).
- <sup>5</sup>J. S. Eck, D. O. Elliott, W. J. Thompson, and F. T. Baker, *Phys. Rev. C* **16**, 1020 (1977).
- <sup>6</sup>W. Brückmer, D. Husar, D. Pelte, K. Traxel, M. Samuel, and U. Smilansky, *Nucl. Phys.* **A281**, 159 (1974).
- <sup>7</sup>F. Todd Baker, Alan Scott, T. P. Cleary, J. L. C. Ford, E. E. Gross, and D. C. Hensley, *Nucl. Phys.* **A321**, 222 (1979).
- <sup>8</sup>Y. Abrall, G. Baron, E. Caurier, and G. Monsonogo, *Phys. Lett.* **30B**, 376 (1969).
- <sup>9</sup>G. J. Stephenson and M. K. Banerjee, *Phys. Lett.* **24B**, 209 (1967).
- <sup>10</sup>Y. Abrall, G. Baron, E. Caurier, and G. Monsonogo, *Phys. Lett.* **26B**, 53 (1968).
- <sup>11</sup>A. S. Davydov and G. F. Filippov, *Nucl. Phys.* **8**, 237 (1958).
- <sup>12</sup>T. R. Ophel and A. Johnston, *Nucl. Instrum. Methods* **157**, 461 (1978).
- <sup>13</sup>J. G. Cramer, R. M. DeVries, D. A. Goldberg, M. S. Zisman, and C. F. Maguire, *Phys. Rev. C* **14**, 2158 (1976).
- <sup>14</sup>M. A. Preston and R. K. Bhaduri, *Structure of the Nucleus* (Addison-Wesley, Reading, Mass., 1975), p. 356.
- <sup>15</sup>G. R. DeMille, T. M. Kavanagh, R. B. Moore, R. S. Weaver, and W. White, *Can. J. Phys.* **37**, 1036 (1959).
- <sup>16</sup>P. M. Endt and C. van der Leun, *Nucl. Phys.* **34**, 1 (1962).
- <sup>17</sup>F. Todd Baker, private communication.
- <sup>18</sup>R. M. DeVries and M. R. Clover, *Nucl. Phys.* **A243**, 528 (1975).
- <sup>19</sup>W. J. Thompson and J. S. Eck, *Phys. Lett.* **67B**, 151 (1977).
- <sup>20</sup>J. S. Eck and W. J. Thompson, in *Nuclear Reactions Induced by Heavy Ions*, edited by R. Bock and W. R. Hering (North-Holland, Amsterdam, 1970), p. 85.
- <sup>21</sup>D. L. Hendrie, *Phys. Rev. Lett.* **31**, 478 (1973).
- <sup>22</sup>T. Tamura, *Nucl. Phys.* **73**, 241 (1965).
- <sup>23</sup>N. M. Clarke, *J. Phys. G* **6**, 865 (1980).